scientific reports

Check for updates

OPEN

Spectroscopic investigation of two xanthane dyes and design of a FRET based pesticide sensor

Sangita Majumder[1], Subrata Deb[2], Shazidul Hussain[1], Dibyendu Dey[3], Debajyoti Bhattacharjee[1], Abdullah N. Alodhayb[4], Shamima Hussain[5] & Syed Arshad Hussain[1]✉

Layer-by-Layer (LbL) technique is the simplest and inexpensive method for prepararion of nano-dimensional thin films for tailoring material behavior having wide range of applications including sensors. Here, spectroscopic behavior of two laser dyes Acriflavine (Acf) and Rhodamine B (RhB) assembled onto LbL films have been investigated. It has been observed that both Acf and RhB form stable LbL films. Polyanion polyacrylic acid (PAA) was used to incorporate the Acf or RhB onto the LbL films. Adsorption of Acf and RhB onto PAA were completed within 45 min and 30 min respectively. During LbL film, material loss occurred in case of Acf. It has been demonstrated that such material loss can be minimized by incorporating clay laponite onto the LbL films. Temperature and pH dependant studies indicate that Acf and RhB assembled onto LbL films can be used to design temperature as well as pH sensors. Fluorescence Resonance Energy Transfer (FRET) between Acf and RhB has also been investigated. Interestingly, it has been demonstrated that the energy transfer efficiency can be manipulated using spacer molecules within the Acf and RhB LbL films. Laponite clay can be used to enhance the FRET efficiency, whereas stearic acid (SA) can be used to lower the efficiency. FRET efficiency linearly changes upon exposure of a pesticide pretilachlor at varying concentration. This study indicated that with proper calibration, proposed sensing system can be used to design FRET based pesticide sensor with detection limit of 0.22 ppm.

Keywords FRET, Dyes, Clay, Pretilachlor, PAA, SA

In materials science and technology, thin films are extremely important as they find many applications ranging from electronics to renewable energy. A thin film is a layer of material with a thickness varying from several micrometers to few nanometers[1]. Significant breakthroughs in a number of applications are made possible by this typical arrangement of materials, which permits exact control over material properties. Furthermore, thin films play a crucial role in optoelectronic applications, where they are utilized in lenses[2], lasers[3], sensors[4], memory devices[5,6] and other optical devices viz. filters[7], mirrors[8], anti-reflective coatings[9], anticounterfeiting and mechanochromic application[10,11], Photodynamic therapy[12] etc.

There exists various approaches those can be employed for thin film deposition viz. Langmuir-Blodgett (LB) technique[4], Spin coating[13], LbL deposition[14], electro-deposition[15] etc. Each technique has its own advantages and disadvantages[16]. Among them, LbL technique has been found to be quiet economical and simple over other conventional thin film preparation method. Here, deposition occurs at almost any environment, with great control of film thickness (from nanometers to micrometers) and does not require complex sophisticated equipments[16,17]. In addition, the LbL self-assembly process allows one to control the thickness of materials placed on a variety of surfaces in a precise manner on nanometer-scale through layer upon layer assembly in a sequential manner[18,19]. This technique was first developed by Decher and his co-workers[16]. Initially, the procedure consists of alternating exposure of substrate surfaces to solutions of oppositely charged polymers in solution[20]. Here, ionic attraction between the opposite charges is the main driving force for the multilayer build up[21]. However, subsequently this technique has been used to prepare ultrathin films using low molecular weight dye molecules also[22]. It is worthwhile to mention in this context that the optoelectronic and aggregating

[1]Thin Films and Nanoscience Laboratory, Department of Physics, Tripura University, Suryamaninagar 799022, Tripura, India. [2]Department of Physics, Women's College, Agartala 799001, Tripura, India. [3]Department of Basic science and Humanities, Techno College of Engineering, Agartala 799004, Tripura, India. [4]King Abdullah Institute for Nanotechnology, King Saud University, Riyadh 11451, Saudi Arabia. [5]UGC-DAE-CSR, Kalpakkam Node, Kokilamedu 603104, Tamilnadu, India. ✉email: sa_h153@hotmail.com; sahussain@tripurauniv.ac.in

behaviors in the restricted geometry of thin films are found to change remarkably in comparison to that in solution or bulk[23]. Accordingly, thin films prepared by LbL technique have been found profound applications in a wide range of scientific appliances, which include sensors[24,25], controlled drug delivery[26], FRET[27], surface coatings[25], optoelectronic devices[28], rewritable control of contact electrification[29], biomedical technologies[30] etc.

In the present work, the spectroscopic characteristics of two xanthane dyes viz. Acf & RhB assembled onto ultrathin films using LbL technique at various micro-environments as well as varying the film forming parameters have been reported. We have also demonstrated the FRET between these two dyes. Energy transfer occurred from Acf (donor) to RhB (acceptor) in the Acf-RhB mixed LbL films and in solution. FRET is an electrodynamic phenomenon; where the transfer of energy from the exited state of a donor to the acceptor[31]. The detailed theoretical background of this energy transfer was sequentially developed by Förster[32,33]. The distance between the donor and acceptor molecules, the relative orientation of their transition dipoles and the extent of spectral overlap between their emission and absorption spectra all affect the rate at which energy is transferred from the donor to acceptor molecule[32–34]. FRET has been utilized to study molecular level interaction owing to its sensitivity to distance of the order of intermolecular order[35]. FRET-based sensing has gained enormous popularity over the recent years because of its advantages, like high sensitivity, quick response time and cost effectiveness. Moreover, FRET based sensors are very specific, which means that their operation in general remains unaffected by the presence of other molecules or other environmental changes and as such they can easily identify a particular analyte or a change. Additionally, FRET sensors are very sensitive and adaptable because they can identify a broad range of biomolecules, chemical analyte and environmental changes[36]. They can be applied to a number of tasks including measuring enzyme activity, detecting protein-protein interactions and monitoring pH changes[31,36]. Also, the optimization of FRET can be controlled by introducing different types of spacer layers in between the donor and acceptor molecules[37]. Also FRET can be manipulated by controlling the donor-acceptor distance as well as orientation. Therefore, it is extremely important to investigate FRET between molecules under various micro-environments. Here in the present work, we tried to optimize the FRET between Acf and RhB incorporating SA as the spacer layer between them. Also clay particles have been incorporated between them to manipulate the FRET efficiency. It has been tried to demonstrate the application of FRET between Acf and RhB to design pesticide sensor.

In the recent years, protection of environment has become a critical issue for the sustainability of life. The extent of various pollutants through a number of anthropogenic activities provides a threat to the environment[38]. Among these pollutants, pesticides are the important entities owing to their applications in crop protection. Pesticides are compounds, primarily used to control weeds, agricultural pests, and other related concerns. On the other hand, they enhance agricultural growth and increase crop productivity. However, pesticides leave residues in agricultural products as well in the environment and contaminate the air, water and soil etc. Accordingly, they enter into the human body which causes serious health hazard. The majority of pesticides are hazardous and uncontrolled use of such chemicals can lead to a decline in the biodiversity of plants, birds and animals. Pretilachlor is a pesticide commonly used during rice cultivation. However, excess use of pretilachlor can be harmful. Even at very low quantities, it is one of the most hazardous compounds and can harm the environment, food, and human health. Hence, exposure of this pesticide should be minimized and optimum use is highly encouraged. For optimum use of pesticides proper management along with regular monitoring of the contamination conditions in the atmosphere, soil and water etc. must be monitored. So, simple, easy to use and highly sensitive sensors with lower detection limit are required.

Gas chromatography and liquid chromatography are the techniques most frequently employed for residue analysis of pretilachlor, both domestically and internationally[39]. A high-performance liquid chromatography-tandem mass spectrometry (HPLC-MS/MS) approach with a detection limit of 0.01 ~ 0.1 μg/kg was developed by Gao et al. to determine pretilachlor in fish[40]. Deka et al. showed that the pretilachlor could be detected using a carbon dot (extracted from water hyacinth) as a fluorescence sensor with a detection limit of 2.9 μM[41].

These techniques are costly and high-end instrumentations are required. Also, they involve complicated operation procedure, time consuming as well as high analytical costs. Liu et al. suggested a pesticide detection method through an indirect enzyme-linked immunosorbent assay (ic-ELISA) to sense the pesticide pretilachlor[42]. However, the procedure requires modifying the target molecule's structure to obtain the immunogen.

Therefore, easy and sensitive method is highly required for the pesticide detection. FRET based sensing system can play a major role in this regard. In the present work, a FRET based pesticide sensor has been demonstrated. The proposed sensor is able to sense the pesticide pretilachlor. This proposed technique is simpler and easy to operate compared to GCMS or GC-ECD based techniques. Also unlike to that of the ic-ELISA method in the proposed FRET based technique, the sample can be used without any further modification. The designed pesticide sensor has been tested to sense pretilachlor and efficient results were obtained.

Also, in the FRET process the ratio between two fluorescence intensities are measured where one fluorescence intensity (donor) increases and the other (acceptor) decreases[43]. Therefore, effect of the presence of any contaminations or junk materials during sensing is automatically minimized. Therefore, FRET based sensing system is highly efficient and sensitive towards the target analytes. It is believed that the proposed FRET based pesticide sensor may be very effective towards sensing and optimum use of pesticides.

As a whole in this work, we have demonstrated the spectroscopic behavior of two dyes Acf and RhB assembled onto LbL films. Different LbL film formation parameters such as interaction time, pH and temperature of solution etc. have been optimized. FRET between Acf and RhB has also been investigated under various micro-environments. Application of FRET in the present system has also been utilized to design FRET based pesticide sensor. Such sensor can be used to sense other chemical contaminants too. Work is going on in our lab in this regard.

Materials and methods

Materials

Xanthane dyes Acf and RhB (Fig.S1 & Fig.S2 of supporting information), PAA, SA were purchased from Sigma Chemical Co. USA and used as received. Distilled water and HPLC grade chloroform were used as solvents. The dyes used in our studies are cationic in nature. The clay mineral used in this work was laponite, and obtained from Laponite Inorganic, UK. The CEC value of 0.739 meq/g was obtained using CsCl, and the size of the clay platelet is less than 0.05 μm[44]. Pretilachlor (Fig.S3 in supporting information) 50% EC (IUPAC Name: 2-chloro-*N*-(2,6-diethylphenyl)-*N*-(2-propoxyethyl)acetamide) was purchased from local market. Different concentrations (0.25 ml/L, 0.5 ml/L, 0.75 ml/L, 1 ml/L) of pretilachlor were prepared using distilled water. Dye solutions were prepared in distilled water. For spectroscopic measurement of the dye films, the concentration was optimized at 10^{-4} M. Distilled water was used to prepare the clay dispersion, which was then magnetically stirred for 24 h and sonicated for 30 min before usage. In all cases, the clay concentration was 2 ppm and the dye concentration was 10^{-4} M for both Acf and RhB. During the fabrication of LbL self-assembled films, PAA was used as a polyanion. The solutions of SA was prepared by dissolving it in HPLC grade chloroform.

UV–Vis absorption and fluorescence spectra measurement

UV–Vis absorption and fluorescence spectra of the solutions and films were recorded by Perkin Elmer Spectrophotometer (Lambda-25), Shimadzu 1800 and Perkin Elmer Fluorescence Spectrophotometer (LS-55) respectively. The excitation wavelength for the fluorescence measurement was 430 nm, which is in proximity to the Acf absorption maximum.

Morphological characterization

Images of the surface morphology of the Acf-RhB films were captured using a Field Emission Scanning Electron Microscopy (FESEM) (Sigma 300 model, Zeiss Pvt., Ltd.) at a 5 kV accelerating voltage both before and after exposure to pretilachlor.

Film preparation

Electrolytic deposition bath of cationic dyes (Acf and RhB, concentration 10^{-4} M) and anionic electrolytic bath of PAA (0.25 mg/mL) were prepared in aqueous solution separately using distilled water. We employ the LbL self-assembly approach for fabricating the Acf and RhB mixed film. Initially, a pure quartz substrate is fully dipped in solutions of anionic PAA and oppositely charged RhB and Acf dye mixure (50:50 volume ratio) alternately. The LbL approach makes use of both the electrostatic and Vander Waals interactions that occur between PAA and cationic dyes as well as the quartz slide. Details about the technique have already been described elsewhere[45]. The quartz slide was immersed in the PAA aqueous solution for thirty minutes. After that, it was removed, given enough time to dry and rinsed in a water bath for two minutes to remove any surplus anion that had attached to the surface. After that, the dry substrate was submerged in a cationic dye combination (RhB + Acf) followed by rinsing in water using the same protocol. PAA, RhB and Acf layer deposition produced a single bi-layer of self-assembled LbL film. We incorporate PAA as a spacer into the LbL thin film. Initially, a single bi-layer self-assembled film of PAA and Acf is prepared using the previously described method. Subsequently, this film is immersed once more in an anionic PAA solution followed by an oppositely charged RhB solution. Now we prepare the LbL thin film where clay is introduced as a spacer. This step is similar as second step but the difference is that here negatively charged clay templates play the role of spacer instead of PAA. Now we prepare the LbL thin film where SA is introduced as a spacer. In this step at first one bi-layer self assembled film of PAA and Acf is prepared followed by deposition of anionic amphiphile SA onto it by LB technique[46]. The SA LB films deposition speed was maintained at 5 mm/min. After that RhB was deposited onto it as described before.

Preparation of Acf-RhB system and detection of pretilachlor

Optimal concentration of Acf and RhB was 10^{-4} M. The mixture of Acf and RhB (50:50 volume ratio) was prepared in distilled water and sonicated for 30 min. In this mixture, pretilachlor of different concentrations (0.25 ml/L, 0.5 ml/L, 0.75 ml/L, 1 ml/L) were added and fluorescence spectra were obtained. Excitation wavelength was kept at 430 nm. It has been observed that due to addition of pretilachlor, FRET efficiency increases and the spectra has slightly shifted from 578 nm to 590 nm (Fig. 1).

Theoretical considerations of FRET

FRET is a well known distance dependent process where an excited fluorophore (donor) transfers its energy to a neighbouring molecule (acceptor) through non-radiative dipole–dipole interaction[32]. Typically FRET occurs with 1–10 nm range[35]. Because of this distance dependency, FRET efficiency is affected due to even minor changes in the interaction or conformation of molecules. When the donor's emission spectrum and the acceptor's absorption spectrum overlap, energy transfer takes place via dipole-dipole coupling.

T. Förster[32,33,47] developed a quantitative explanation for the non-radiative energy transfer in terms of his famous formula given by

$$k_T(r) = \frac{1}{\tau_D} \times \frac{9000 \ln(10) K^2 \Phi_D J}{128 \pi^5 N_A n^4} \times \frac{1}{r^6} = \frac{1}{\tau_D} \left(\frac{R_0}{r} \right)^6 \quad (1)$$

Hence,

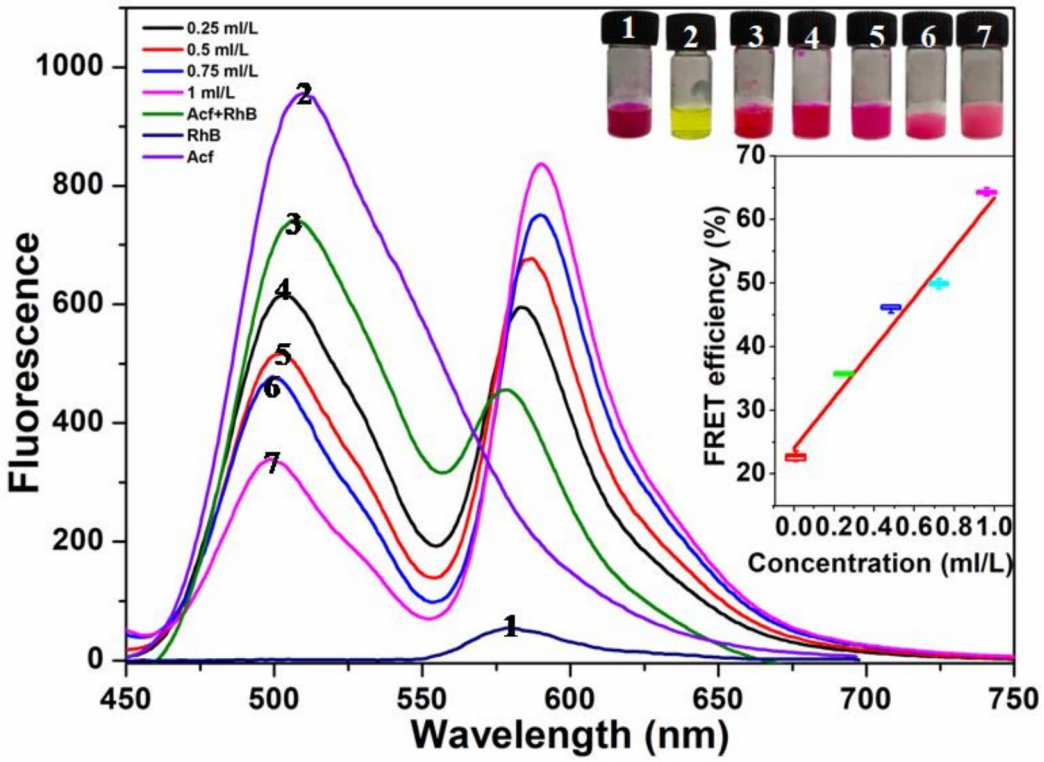

Fig. 1. Fluorescence spectra of pure Acf, pure RhB, Acf + RhB in presence of pretilachlor of different concentrations (0.25 ml/L, 0.5 ml/L, 0.75 ml/L, 1 ml/L). Inset shows the variation of FRET efficiency with pretilachlor concentration. Also the photographs of the Acf & RhB mixture in presence of pretilachlor at different concentrations are shown in the inset.

$$R_0 = \left[\frac{9000\ln(10)\,K^2\Phi_D J}{128\pi^5 N_A n^4}\right]^{\frac{1}{6}} \tag{2}$$

Where, $k_T(r)$ is the rate of energy transfer from donor to acceptor and r is the distance from the donor to acceptor. The distance between the donor and the acceptor is called Förster radius (R_0), where the FRET efficiency is 50%. K^2 is the orientation factor of transition dipole moment between acceptor and donor, n is the refractive index of medium, N_A is the Avogadro number, Φ_D is the fluorescence quantum yield of donor in absence of acceptor, τ_D is the donor's lifetime in the absence of the acceptor and J is the spectral overlap integral as given in Eq. 3 as follows.

Spectral overlap integral $J(\lambda)$ is herein given by,

$$J(\lambda) = \int_0^\infty F_D(\lambda)\,\varepsilon_A(\lambda)\,\lambda^4\,d\lambda \tag{3}$$

Where $F_D(\lambda)$ is the donor emission profile and $\varepsilon_A(\lambda)$ is the acceptor extinction coefficient.

Therefore, Eq. 2 can be re-written as

$$R_0 = 0.2108\,[K^2 n^{-4}\Phi_D J(\lambda)]^{1/6} \tag{4}$$

The FRET efficiency can be defined in terms of Förster radius (R_0) and the rate of energy transfer $k_T(r)$ as follows –

$$E = \frac{k_T(r)}{k_T(r) + \frac{1}{\tau_D}} = \frac{R_0^6}{R_0^6 + r^6} \tag{5}$$

Hence, intermolecular distance (r) between donor and acceptor can be expressed as

$$r = R_0 \left[\left(\frac{1}{E}\right) - 1\right]^{1/6} \tag{6}$$

FRET efficiency can also be expressed in terms of donor lifetime as well as emission profile as follows[48] –

$$E = 1 - \frac{\tau_{DA}}{\tau_D} = 1 - \frac{F_{DA}}{F_D} \tag{7}$$

Where F_D and F_{DA} are the fluorescence intensities of the donor in the absence and presence of acceptor respectively. τ_D and τ_{DA} are the fluorescence lifetime of the donor in the absence and presence of acceptor respectively.

In the present work, Eqs. 3, 4, 6 and 7 have been used to calculate the values, $J(\lambda)$, R_0, r and E respectively.

Results and discussions

UV-Vis absorption and steady state fluorescence spectroscopy

Figure 2(a) and Fig. 2(b) show the normalized absorption and fluorescence spectra of Acf in solution, microcrystal and LbL film. The absorbance spectrum of Acf in aqueous solution shows an intense band at 449 nm, which is assigned due to the Acf monomer. Acf microcrystal and LbL film absorption spectrum are almost similar to that of solution absorption spectrum. Although some broadening of absorption band is observed. This may be due to the change in the micro-environment as well as trace of aggregate formation when Acf molecules are transferred onto restricted geometry of microcrystal and LbL films[23]. The fluorescence peak of Acf solution is observed at 510 nm, which is assigned due to the Acf monomer. Acf fluorescence band is found to be shifted towards longer wavelength at 521 nm for LbL films and 537 nm for microcrystal. This may be due to the tendency of aggregation when Acf molecules are transferred onto solid support[23]. Observed difference in peak position in case of LbL

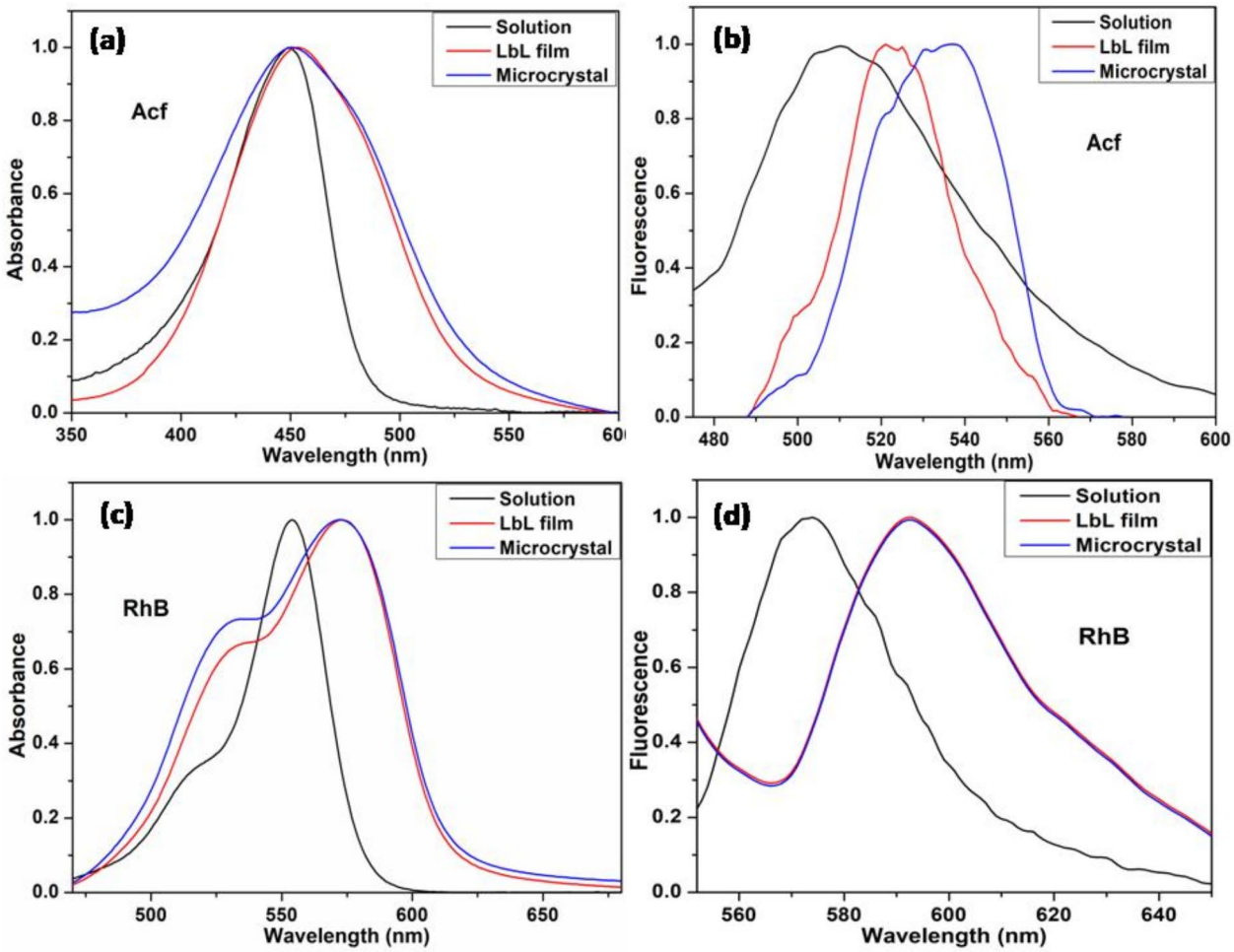

Fig. 2. (**a**) UV-Vis absorption and (**b**) Fluorescence spectra of Acf in solution, LbL film and microcrystal. (**c**) UV-Vis absorption and (**d**) Fluorescence spectra of RhB in solution, LbL film and microcrystal. Excitation wavelengths for fluorescence measurement, were 430 nm and 550 nm for Acf and RhB respectively.

and microcrystal may be due to the difference in order of aggregation in two cases. This may be due to the fact that molecules are more organized and uniform in LbL film compared to that in microcrystal[49].

Figure 2(c) and Fig. 2(d) show the normalized absorption and fluorescence spectra of RhB in solution, microcrystal and LbL film. RhB absorption spectrum possess prominent intense 0–0 band at 554 nm along with a weak hump at 520 nm which is assigned due to the 0–1 vibronic transition[50]. RhB absorption bands in microcrystal as well as in LbL films are found to be red shifted with bands at 573 nm and 574 nm. The RhB fluorescence spectrum shows prominent band at 574 nm which is assigned due to the RhB monomeric emission. The RhB fluorescence band is found to be red shifted to 592 nm in LbL film and microcrystal. This may be due to the tendency of aggregation when the RhB molecules are transferred to solid films[23]. Here both absorption and fluorescence spectra for RhB in LbL film and microcrystal are almost similar. This indicate that the order of RhB aggregates may be almost similar in both microcrystal and LbL films.

Adsorption kinetics during LbL film formation

LbL film deposition is primarily governed by the electrostatic interaction between oppositely charged molecules[16]. This interaction is a time dependant process[51]. In order to monitor the adsorption kinetics, LbL films of both Acf and RhB have been deposited onto quartz substrate by varying deposition time and absorbance of the concerned films have been measured[16]. Figure 3(a) and Fig. 3(b) show the plot of the absorbance maximum of the LbL films deposited at different times starting from 5 min to 55 min for Acf and RhB respectively. Inset of Fig. 3(a) and Fig. 3(b) show the corresponding absorption spectra. From the figures, it is observed that the absorbance increases initially with the deposition time for both Acf and RhB. However, after certain time absorbance reaches to its maximum. In case of Acf, absorbance reaches to its maximum with deposition time 45 min. Whereas, for RhB, the absorbance reaches to its maximum with deposition time 30 min. After that the intensity becomes almost constant and remains the same for all the films deposited with higher deposition times. It may be mentioned in this context that during LbL film deposition initilally a polyanion PAA is deposited onto the quartz slide[49]. This makes the film surface negatively charged. After that the film is dipped onto either Acf or RhB solution. Since Acf and RhB are cationic in nature, they are adsorbed onto the film through electrostatic interaction with PAA[16]. Number of Acf or RhB molecules adsorbed increases with time accordingly the absorbance increases with time initially. However, after certain time (45 min for Acf and 30 min for RhB) almost all PAA molecules are attached with the Acf or RhB and no PAA molecule remains free in the film to adsorb Acf or RhB molecules futher. Here, the ideal film deposition time is estimated to be 45 min for Acf and 30 min for RhB. Accordingly, deposition time for all the films were kept constant at 45 and 30 min for one bi layer Acf and RhB films respectively for further studies.

Layer effect study

LbL self assembly is a simple and useful technique to prepare multilayer films through alternate deposition of cationic and anionic materials[52]. During the multilayer film deposition, it is important to monitor the film growth with increase in layer number. It is very much relevant to mention here that there are mainly two buildup mechanisms viz. linear and exponential during the electrostatic LbL assembly[17]. Linear growth is the simplest one in which the thickness and mass of the film increase linearly with the number of deposited bilayers and each polyelectrolyte layer interpenetrates only with the adjacent ones[16]. However, during exponential growth, there is high chain mobility, generally in the direction normal to the film and in the plane of the film leading to the

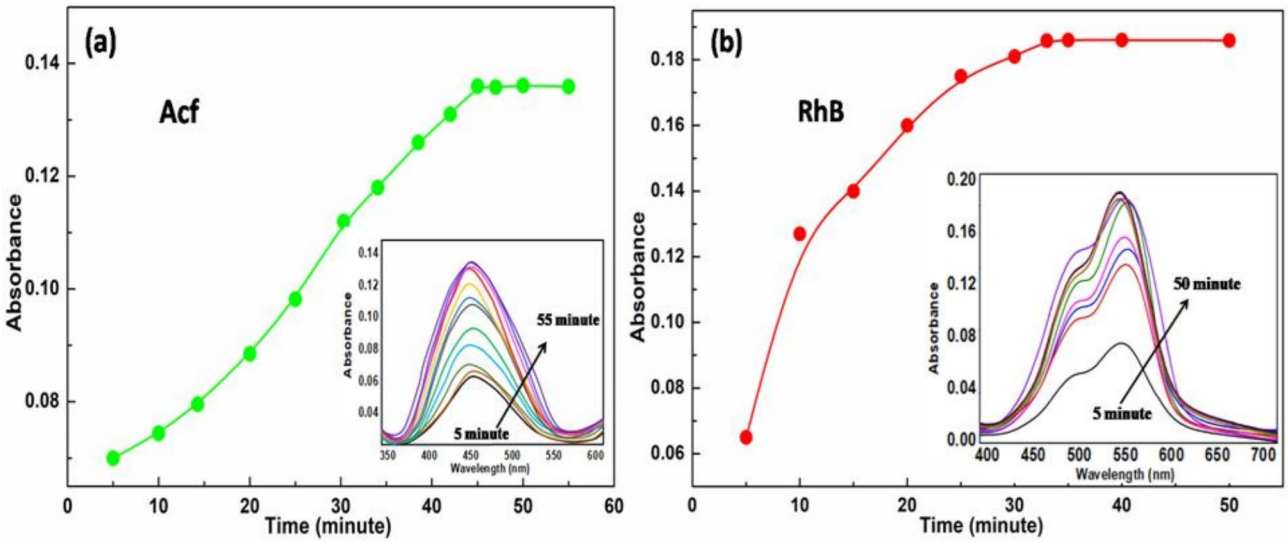

Fig. 3. Plot of absorbance as a function of deposition time for (**a**) Acf and (**b**) RhB. Inset shows corresponding absorption spectra.

diffusion of at least one of the constituents in and out of the film architecture with the subsequent exponential thickness increase with the number of deposited bilayers[53]. The growth mechanism of multilayer films prepared from poly (L-lysine) (PLL) as polycation has been reported to be exponential[17,54,55]. Also it is well known that the film thickness effects the opto-electronic behavior to a certain extent. Accordingly, in the present case, we have investigated the spectroscopic behavior of Acf and RhB assembled onto LbL films with varying layer number. The UV-vis absorption spectra of different layered PAA-Acf and PAA-RhB LbL self assembled films are shown in Fig. 4(a) and Fig. 4(b) respectively. From Fig. 4, it has been observed that the absorbance of both Acf (Fig. 4a) and RhB (Fig. 4b) increases systematically with increase in layer number. This is an indication that almost uniform deposition of Acf and RhB occurred in the multilayer LbL films with increasing layer numbers. Also the absorption band pattern are almost similar for different layered LbL films for both Acf and RhB except an increase in absorbance intensity. This indicates that the organization/aggregation pattern remains almost similar for both Acf and RhB in the different layered LbL films irrespective of layer number. Also from the insets of Fig. 4(a) and Fig. 4(b), we definitely can make a conclusive remarks regarding the linear nature of growth in case of multilayer LbL films.

Effect of temperature and pH

It has been observed that temperature play crucial role during absorption of organic molecules onto LbL films[56]. In the present case also effect of temperature on the formation of Acf-PAA and RhB-PAA LbL films have been investigated. In order to do that, the temperature of concerned solutions have been varied with in the range of 30˚C-60˚C during LbL film formation. LbL films were deposited during both heating and cooling cycle and absorption spectra were recorded for all the cases. Figure 5(a) and Fig. 5(b) show the plots of maximum absorbance intensities as a function of temperature for both Acf and RhB. Systematic decrease in absorbance is observed for both Acf and RhB with increasing temperature. However, the position of maximum absorbance for both Acf and RhB remained almost same. This indicates that there will be almost no structural change in Acf and RhB with temperature.

However, reversible phase transition or reorientation of PAA may occur with change in temperature[57]. It has been reported that PAA grafted with Poly(N, N-dimethylacrylamide) (PDMA) showed a liquid-liquid phase transition upon heating[58]. Sinek et al. reported that the PAA chains decompose at temperatures between 230 and 300 °C and at lower temperature conformational / phase change occurred only[57]. In the present case, the temperature range under investigation was 30 to 60 ^{0}C. So there will be no possibility of permanent degradation / deformation of PAA structures rather phase change or reorientation is highly desirable. This may affect the interaction between PAA with either Acf or RhB and as such number of Acf or RhB molecules adsorbed onto LbL films decreased. Also, there may be aggregation of Acf or RhB in the LbL films deposited at higher temperature due to PAA conformational change[59].

It has been reported that thermal degradation, phase change as well as change in aggregation pattern occurred in PAA upon change in temperature[56,60]. Some probable modification in the aggregation pattern of PAA molecules upon heating may also be responsible for a declination towards PAA-Acf and PAA-RhB interactions. Chain association and dissociation of the polymer PNIPAAM in aqueous environment upon heating-cooling cycle have also been reported[61]. Similar chain association and dissociation of PAA may affect the interaction of PAA with cationic Acf and RhB in LbL films[45].

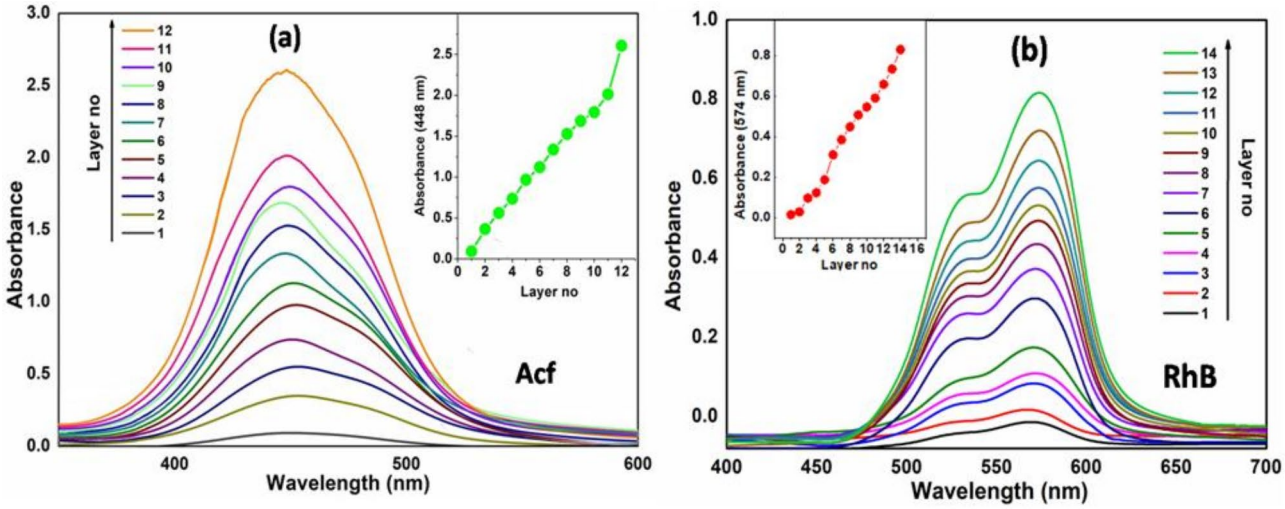

Fig. 4. Absorption spectra of (**a**) Acf and (**b**) RhB in LbL films with increasing layer number. Inset shows the plot of the absorbance as a function of layer number.

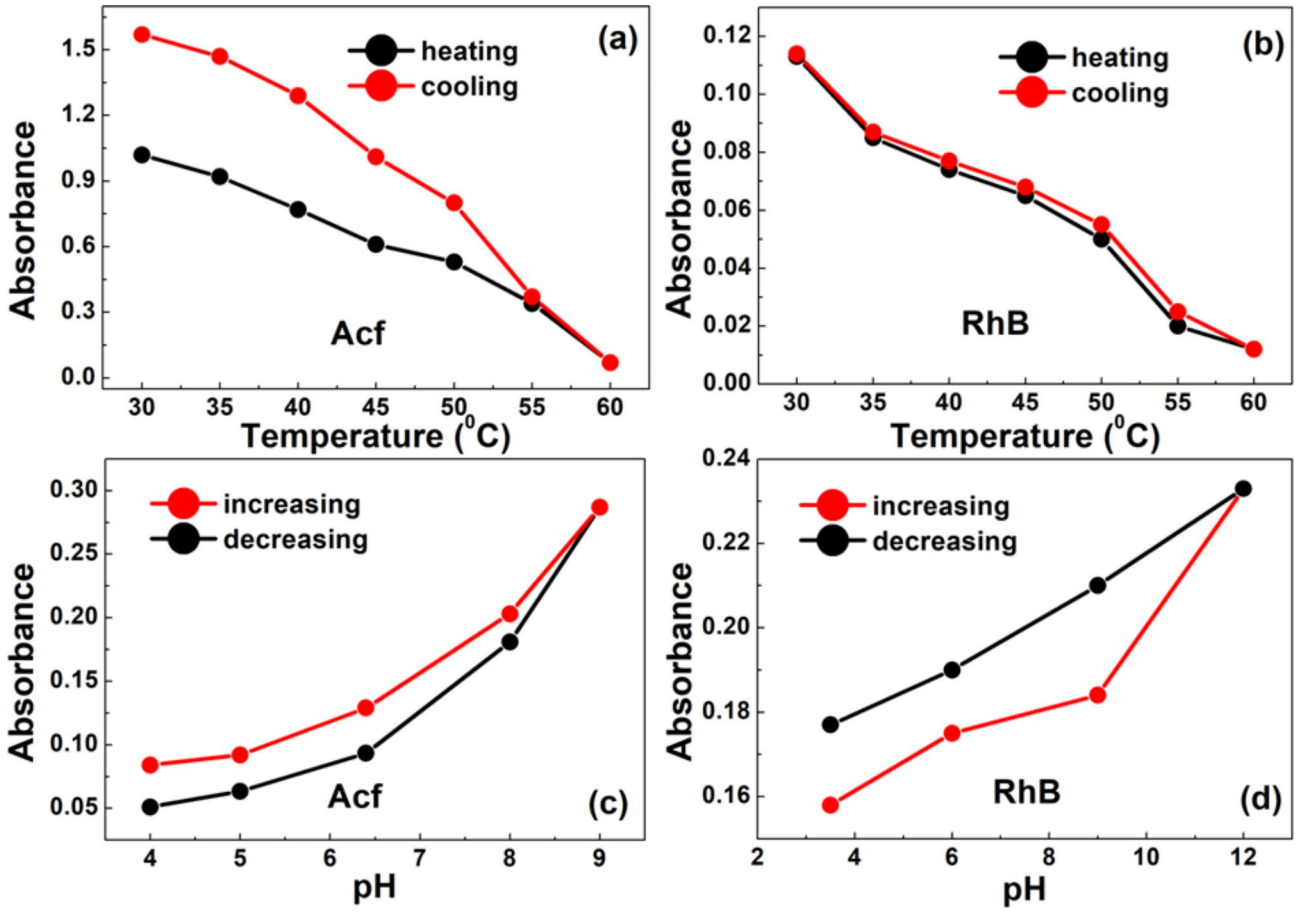

Fig. 5. Variation of absorption intensity of (**a**) Acf and (**b**) RhB with increasing and decreasing temperature. Variation of absorption intensity of (**c**) Acf and (**d**) RhB with increasing and decreasing pH.

On the other hand, absorbance of the LbL films measured during cooling process increases systematically (Fig. 5a and b). Interestingly, large hysteresis is observed for Acf in LbL films. However, RhB absorbance did not show any marked hysteresis. Observed hysteresis with increase in Acf absorbance at a higher intensity might be due to the phase restoration and reorientation of PAA in such a way that favourable interaction between Acf and PAA occurred leading large number of Acf assembled onto LbL films. Also, the reorientation / conformational change upon cooling may decrease / minimize the Acf aggregation. This may also result in enhancement of Acf absorbance.

However, in case of RhB, almost no hysteresis is observed. This also suggests that the phase change / conformational change in case of poly-electrolyte PAA upon heating-cooling cycle are reversible in nature. This also negate any structural deformation of PAA. Therefore, it may be concluded that change in the preferential orientation of Acf molecule occurred during the process of cooling, which in turn effect the Acf adsorption in LbL flms. It has been reported that Chikago Sky Blue also showed similar hysteresis upon heating-cooling process[62].

The dye Acf and polymer PAA used in the present investigation are highly pH sensitive[60,63]. The presence of central nitrogen atom within the Acf structure makes it pH sensitive. On the other hand, polymer show responsive phase change[64]. Also the association-dissociation as well as aggregation behavior of polymer are highly dependant on pH. Accordingly, Acf-PAA and RhB-PAA LbL films have been prepared at varying pH range and their absorption spectra have been recorded.

Figure 5(c) and Fig. 5(d) show the plot of absorbance of one bilayer Acf-PAA and RhB-PAA LbL films deposited using Acf and RhB solutions of varying pH. Interestingly, it is observed that the intensity of absorbance spectra varies significantly with pH. The intensity of absorption bands increases with increasing pH for both Acf and RhB. This may be due to the increase in OH^- ions within the PAA film, which provides a larger electrostatic attraction of PAA with cationic Acf and RhB. Also the pH induced change in association/aggregation nature as well as phase change of PAA in LbL film may affect the interaction of PAA with Acf and RhB during LbL film formation[49]. Interestingly, large hysteresis is observed for both Acf and RhB in the LbL film formed during decreasing pH. This may be due to non-reversible nature of change of PAA in two cases during increasing and decreasing pH. Also the difference in hysteresis for Acf and RhB may be due to difference in re-orientation as well as ionization nature of Acf and RhB during pH change. Observed almost linear chage in absorbance with increasing pH may be useful for designing pH sensor in future.

Material loss during LbL film formation

The binding between two oppositely charged molecules in LbL films is of fundamental importance in relation to any technological applications. If the binding is weak then during the subsequent deposition out of these two molecules, a particular type of molecules can come out of the multilayer film, which is replicated by a decrease in the absorbance intensity. If no such decrease in the absorbance intensity is seen between subsequent deposition onto the solid substrate, then it can be said that the binding between two oppositely charged molecules is strong and there is almost no material loss during multilayer growth. In order to have an idea about the binding behaviour and the material loss during PAA-Acf and PAA-RhB LbL film deposition on to a quartz substrate, we have recorded UV-Vis absorption spectra of these films after dipping in dye solution and as well as in PAA solution.

Figure 6(a) shows the plot of intensity of Acf absorption maximum at 450 nm peak as a function of number of deposited layers either Acf or PAA. The above points represent absorption intensity at 450 nm recorded after the deposition of the Acf layer and below points represent the absorption intensity at 450 nm after each layer of PAA deposition. From the figure, it is evident that the absorbance increases after each Acf layer deposition and decreases after deposition of each PAA layer. Interestingly, there is no change as far as the position of peak is concerned. So, from these observations, it can be confirmed that some of the Acf molecules may come out of the Acf-PAA film when the same is dipped in the PAA solution. This implies that the binding between PAA and Acf molecules is not very strong in the Acf-PAA films and as such some Acf molecules are coming out during deposition in PAA solution as evidenced from Fig. 6(a). Figure 6(b) shows the similar study for RhB-PAA LbL films and from the figure, it is obvious that there is almost no such decay of absorbance intensity after deposition of film in PAA solution. Accordingly, we may conclude that RhB molecules did not come out of the film during PAA deposition. This also suggests that the electrostatic interaction between RhB and PAA molecules in RhB-PAA film is much stronger than that in between Acf and PAA molecules in Acf-PAA film. In order to improve the binding between Acf and PAA molecules in Acf-PAA film, we have incorporated nano-clay laponite during Acf-PAA LbL film formation. Corresponding plot is depicted in Fig. 6(c). From the figure, it is observed that the Acf molecules do not come out of the film in presence of clay. This is evidenced from the fact that the intensity of the absorbance peak does not show any decrease after depositing the same in PAA solution in presence of clay. In such a case, the interaction between anionic clay particles and cationic Acf molecules is much stronger and as a result the PAA-Clay-Acf LbL films are fabricated almost without any material loss.

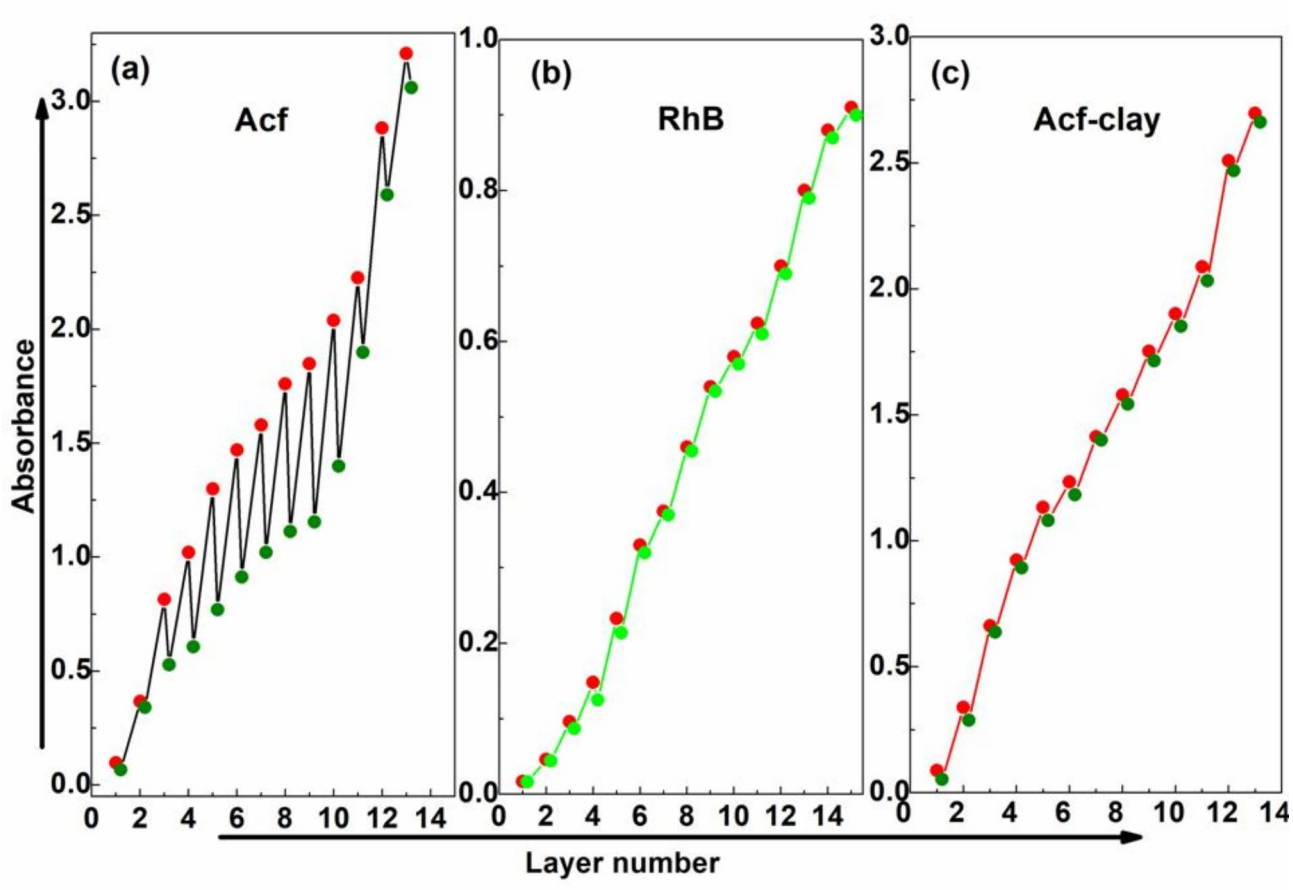

Fig. 6. Plot of absorbance intensity as a function of deposited layers in PAA to study the material loss for (**a**) Acf (**b**) RhB (**c**) Acf in presence of clay.

FRET between Acf and RhB

FRET is the non-radiative transfer of energy from a molecule (donor) to another molecule (acceptor)[31]. FRET can be used as a tool to investigate supramolecular organization at moleculer level distance as well as to design various sensors[35,36]. In order to occur FRET between two fluorophore there must be overlapping of the donor emission and acceptor absorption spectra[33,34]. Also the alignment of their dipoles as well as proximity between them play important role[32].

In the present case, Acf fluorescence and RhB absorption have sufficient overlap (Fig.S4 of supporting information). Also both the molecules show prominent fluorescence. Accordingly, it has been planned to investigate possibility of FRET between them. Here Acf acts as an energy donor and RhB acts as an energy acceptor. Also both the dyes are highly fluorescent, which are the prerequisite for FRET to occur[31]. In few of our previous reports, we have explained the energy transfer between Acf and RhB in solution[31,65,66].

In order to investigate the possible FRET between Acf and RhB, the fluorescence spectra of Acf, RhB and (Acf + RhB) mixture in 50:50 volume ratio are measured with exciting wavelength at 430 nm (close to absorption maximum of Acf). The excitation wavelength was selected approximately to excite the Acf molecules directly and to avoid or minimize the direct excitation of the RhB molecules.

Figure 7 reveals the presence of a strong and prominent peak at around 510 nm in case of Acf. But in case of RhB, the fluorescence band is found to be at around 574 nm and also very weak in intensity. The observed weak intensity of fluorescence band of pure RhB solution justifies towards a smaller contribution of direct excitation of the RhB molecules with the chosen excitation wavelength $\lambda_{ex} = 430$ nm. However, the fluorescence spectra of Acf and RhB mixture in 50:50 volume ratio is quiet interesting. In case of fluorescence spectrum of Acf and RhB mixture, it is observed that the band at 510 nm (supposed to be for Acf) is found to be decreasing while the band at 574 nm (supposed to be for RhB) is increasing prominently compared to their pure counterpart. Here, the Acf emission intensity decreases due to the transfer of energy from Acf molecules (donor) to the RhB molecules (acceptor)[34]. This transferred energy excites more RhB molecules in the solution, which is added to the original RhB fluorescence. As a result the RhB fluorescence intensity gets sensitized. The excitation spectra Acf-RhB mixed thin films was measured with monitoring emission wavelength fixed at Acf fluorescence maximum

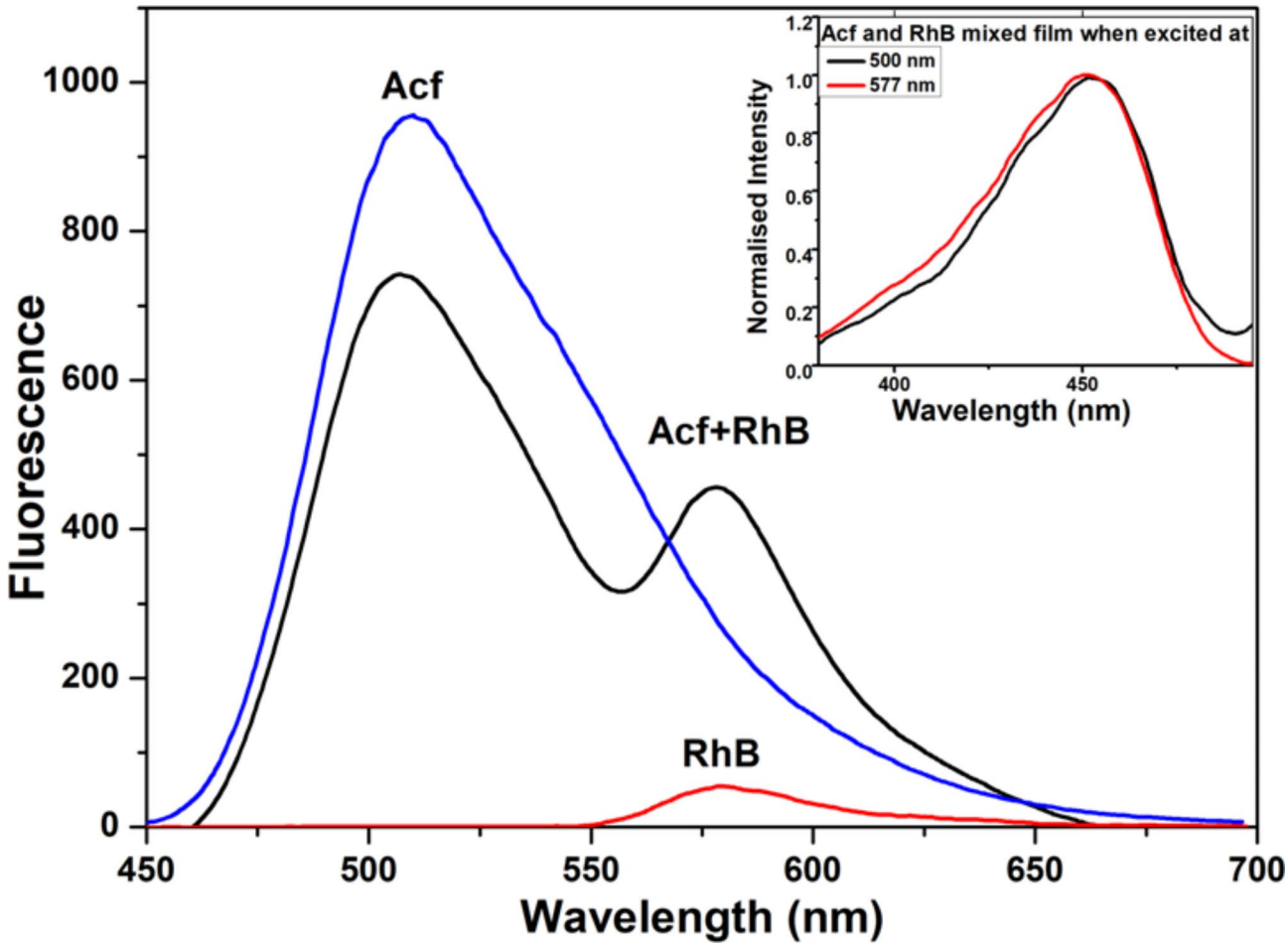

Fig. 7. Fluorescence spectra of pure Acf, pure RhB and Acf + RhB mixture (50:50 volume ratio) in solution. Inset shows the excitation spectra of Acf and RhB at the emission wavelength monitored at 500 nm (Acf emission maximum) and 577 nm (RhB emission maximum).

(500 nm) and for RhB fluorescence maximum (577 nm). Interestingly, both the excitation spectra are almost similar and possess characteristic absorption bands of Acf monomers (Inset at Fig. 7).This clearly confirms that the enhnachment of fluorescence intensity in RhB mainly arises due to the light absorption by Acf molecules and subsequent transfer at the same to RhB monomer.

Effect of different spacer molecules on FRET between Acf and RhB

FRET is pre-dominantly a distance dependent phenomenon and as such FRET efficiency is found to depend on many parameters viz. distance between donor and acceptor (typically in between 1 and 10 nm), the spectral overlap and the relative orientation of donor and acceptor dipole moment[35]. Choice of appropriate spacer molecules may help to manipulate distance between the donor-acceptor fluorophores and may be very useful to optimize the FRET process.

To investigate the effect of different spacer groups on the FRET between Acf and RhB, we have studied the effect of PAA, SA and clay as a spacer layer between Acf and RhB. In Fig. 8, we have shown the fluorescence spectra of Acf and RhB mixed thin films prepared under various conditions. We have inserted three different spacers PAA, SA, Clay between Acf and RhB layers and measured the FRET efficiency between Acf and RhB in all the cases. All the values of FRET parameters are calculated by using Foster theory and have been tabulated in Table 1[32]. Details of FRET parameter calculation procedure has been reported elsewhere[67]. From the Table 1, it is observed that the FRET efficiency was 22.52% for Acf and RhB mixture without any spacer molecules with an intermolecular separation (r) of 7.28 nm. When PAA molecules were used as spacer layer in between Acf and RhB in LbL film, the FRET efficiency decreases to 19.67%. In case of SA molecules (both 1 layer and 3 layers), the FRET efficiency gets reduced to 15.60% and 7.33% respectively with intermolecular separation as 7.48 nm and 8.00 nm respectively. Interestingly, with an increase in the number of layers of SA from 1 to 3, the FRET efficiency gets largely affected and is reduced by 61% approximately compared to its value without any spacer molecules.

On the other hand, in case of clay as the spacer, the FRET efficiency is larger (25.71%) with the lowest intermolecular separation of 7.11 nm. It is worthwhile to mention in this context that clay particles are negatively charged and have layered structure with a cation exchange capacity[68,69]. Both the dyes Acf and RhB under investigation are positively charged. Accordingly, they are adsorbed on to the clay layers[31,70]. Therefore,

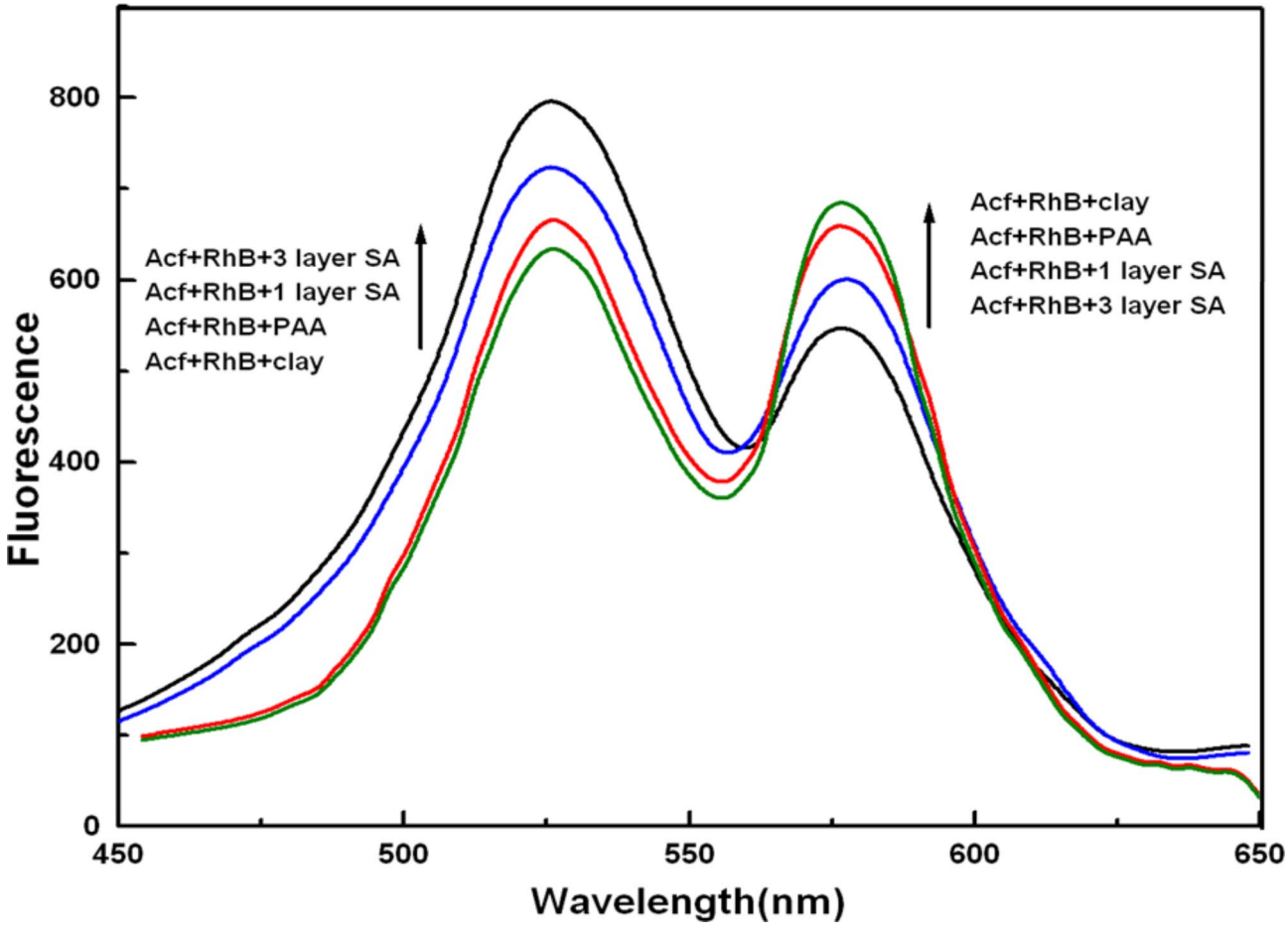

Fig. 8. Fluorescence spectra of (Acf + RhB) in presence of PAA, (Acf + RhB) in presence of SA of 1 layer, (Acf + RhB) in presence of SA of 3 layers, and (Acf + RhB) in presence of clay.

Sample	J(λ)X10^{15}m^{-1}cm^{-1}nm^4	R_0(nm)	r(nm)	FRET efficiency (E%)
Acf + RhB	3.82	5.93	7.28	22.52
Acf+(PAA) + RhB	3.27	5.78	7.32	19.67
Acf+(1 layer SA) + RhB	2.85	5.65	7.48	15.60
Acf+(3 layer SA) + RhB	1.82	5.24	8.00	07.33
Acf+(clay) + RhB	4.12	5.96	7.11	25.71

Table 1. Variation of FRET efficiencies and other parameters between Acf and RhB, with different spacers like PAA, 1 layer SA, 3 layers SA and clay.

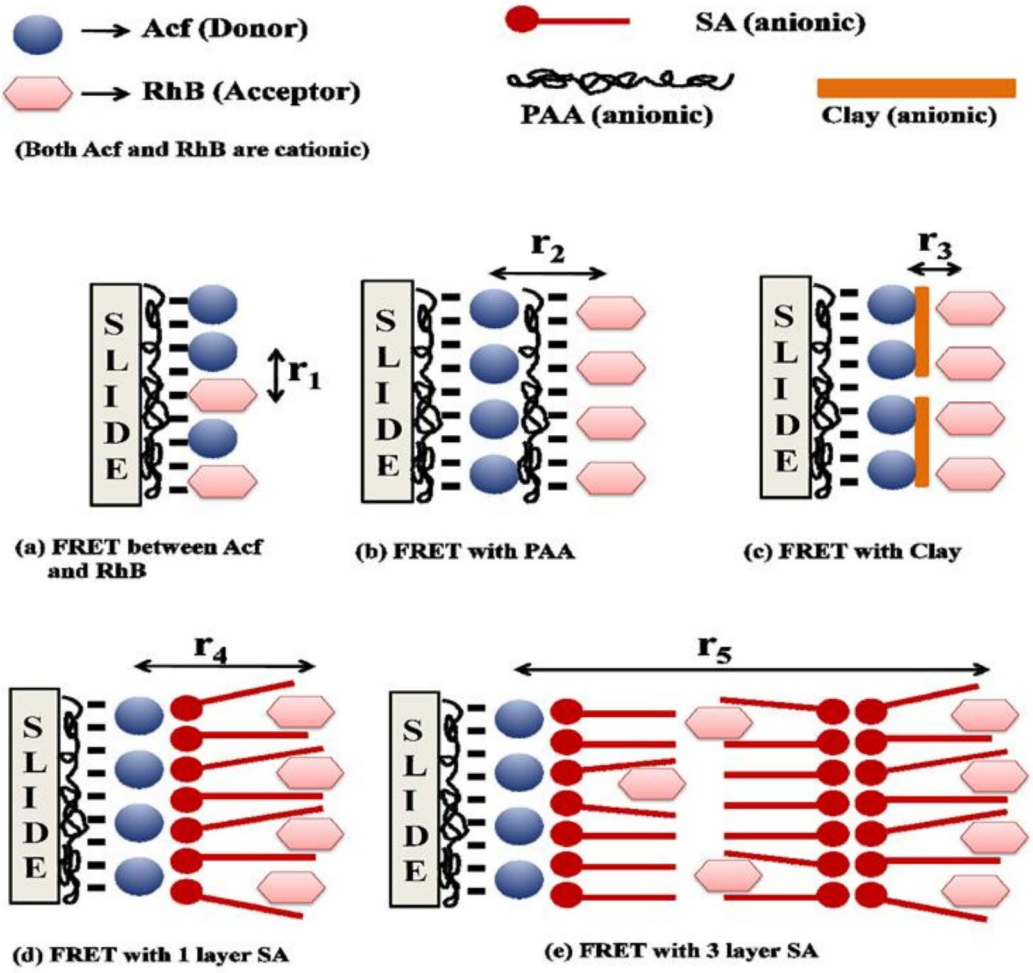

Fig. 9. Schematic representations of FRET between Acf and RhB (**a**) without any spacer (**b**) with PAA as spacer (**c**) with clay as spacer (**d**) with 1 layer of SA as spacer (**e**) with 3 layers SA as spacer.

clay particles play an important role in determining the concentration of the dyes on their surfaces or to make possible close interaction between donor and acceptor. The variation of intermolecular separation between Acf and RhB has been shown schematically in the next part of the manuscript.

Schematic diagram

A schematic diagram shows the organization of Acf and RhB on to thin film in presence and absence of different spacers molecules. Figure 9(a) shows the incorporation of cationic Acf and RhB on to anionic polymer (PAA) back bone and there is no spacer between Acf and RhB. In this case the FRET efficiency is 22.52%. A spacer polymer PAA has been introduced in between Acf and RhB as depicted in Fig. 9(b). As a result, the intermolecular separation between Acf and RhB increases, resulting a decrease in FRET efficiency (19.67%). Similarly in Fig. 9(d) and Fig. 9(e) SA of different layers (1 and 3 layers respectively) have been used as spacer between Acf and RhB and FRET efficiency decreases further with increasing inter molecular separation. But in

presence of clay (Fig. 9(c)) the intermolecular separation between Acf and RhB decreases which results in an increase in FRET efficiency (25.71%). In presence of clay, the dyes are adsorbed by cation exchange reaction on to the clay surface and accordingly the distance between Acf and RhB decreases as shown in the Fig. 9(c). This in turn can increase the energy transfer efficiency.

Sensing of pretilachlor by FRET

In the earlier sections of the manuscript, we have demonstrated FRET between Acf and RhB as well as tried to optimize the same. Here, we have extended our studies to apply the FRET between Acf and RhB to detect a pesticide. Interestingly it has been observed that the present FRET system is capable of detecting one common pesticide viz. pretilachlor.

Figure 1 shows the fluorescence spectra of pure Acf, pure RhB, and Acf-RhB mixture in presence of pretilachlor at different concentrations (0.25 ml/L, 0.5 ml/L, 0.75 ml/L, 1 ml/L). All the fluorescence spectra were recorded with excitation wavelength 430 nm i.e., close to Acf absorption maximum in order to avoid direct excitation of RhB. Interestingly, it has been observed that RhB fluorescence intensity systematically increases with increase in pretilachlor concentration. On contrary, the Acf fluorescence intensity decreases with increase in pretilachlor concentration. This is a clear indication that FRET between Acf and RhB systematically increased due to the presence of pretilachlor. In order to quantify the FRET in presence of pretilachlor, different FRET parameters like intermolecular separations, FRET efficiencies etc. have been calculated and shown in Table 2. It has been observed that FRET efficiency between Acf and RhB was 22.52% in absence of Pretilachlor. Interestingly, FRET efficiency increased in presence of pretilachlor. FRET efficiency increased almost linearly with pretilachlor concentration (inset of Fig. 1). Maximum FRET efficicency was 64.56% for pretilachlor concentration of 1 mL/L.

FRET is a distance dependant phenomenon and typically effective within the 1–10 nm range[71]. Along with other parameters, the FRET efficiency largely depends on the donor-acceptor distance as well as on the relative orientations of the two dipoles[72]. With decrease in donor-acceptor distance, FRET efficiency increases. Also increase in spectral overlap integral enhances the FRET efficiency.

In the present case, the distance between Acf and RhB decreases in presence of the pesticide pretilachlor (Table 2). Also, the spectral overlap integral increases in presence of the pesticide (Table 2). This may be due to the fact that in presence of pesticide simultaneous hydrogen boding between the pesticide pretilachlor and the dyes Acf as well RhB.

The carboxyl group (-COOH) of Acf may form hydrogen bonding with the oxygen or chlorine of pretilachlor, whereas, the amino group ($-NH_2$) of RhB may form a hydrogen bond with Cl or oxygen of the pretilachlor as shown below (Fig. 10). Accordingly, pretilachlor helps Acf and RhB molecules to come closer resulting an increase in FRET efficiency. Calculated values revealed that distance (r) between Acf and RhB in absence of pretilachlor was 7.28 nm which systematically decreases with increase in pretilachlor concentration (inset of Fig. 1). Also the hydrogen bonding between the pesticides and dyes affected the spectral overlap integral and its value increases with increase in pesticide concentrations (Table 2).

Observed systematic linear increase in FRET efficiency with increase in pretilachlor concentration indagates with proper calibration FRET between Acf and RhB can be employed to design pesticide sensor. The limit of detection of the proposed sensor is found to be 0.22 ppm. Limit of detection has been calculated based on the earlier reports[73].

The designed sensor has been tested for various concentrations of pesticides and for each concentration five independent set of experiments have been done. Almost reproducible results were obtained. The FRET efficiency presented in Table 2 is the average of five measurements. The variation in the FRET efficiency has been shown through box plot (inset of Fig. 1).

FESEM studies

FESEM was used to see the change in morphology of Acf-RhB system in presence and absence of the pesticide pretilachlor. This investigation gives us the visual confirmation of morphology, about how the presence of pesticide pretilachlor affects the Acf-RhB system. Figure 11 (a) and Fig. 11 (b) show the FESEM images of the Acf and RhB mixture before and after pretilachlor exposure. The FESEM image of Acf and RhB films in absence of the pesticide looks like an undivided structure. On the other hand, the FESEM image of Acf and RhB after the exposure of pesticide pretilachlor showed visual marked change (Fig. 11 (b)). It clearly demonstrates a broken plate like or circular discs like structures. This information gives us a compelling visual evidence regarding the occurrence of some marked change in Acf-RhB film morphology when it is exposed to pretilachlor.

Sample	$J(\lambda) \times 10^{15} m^{-1} cm^{-1} nm^4$	R_0(nm)	R (nm)	FRET efficiency (E%)
Acf + RhB	3.82	5.93	7.28	22.52
Acf+(0.25 ml/L of pretilachlor) + RhB	5.094	6.18	6.81	35.64
Acf+(0.5 ml/L of pretilachlor) + RhB	6.1	6.36	6.53	45.97
Acf+(0.75 ml/L of pretilachlor) + RhB	6.53	6.44	6.44	50
Acf+(1 ml/L of pretilachlor) + RhB	7.92	6.65	6.01	64.56

Table 2. Variation of various FRET parameters between Acf and RhB in presence of pretilachlor (pesticide).

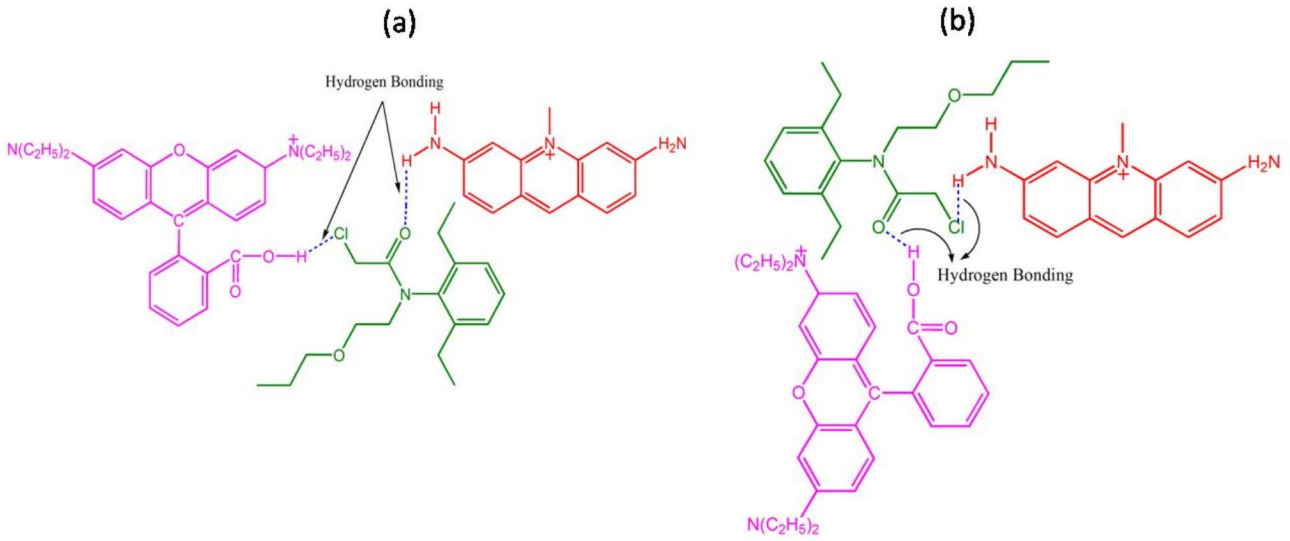

Fig. 10. Schematic of the closer association of Acf and RhB via hydrogen bonding with pretilachlor.

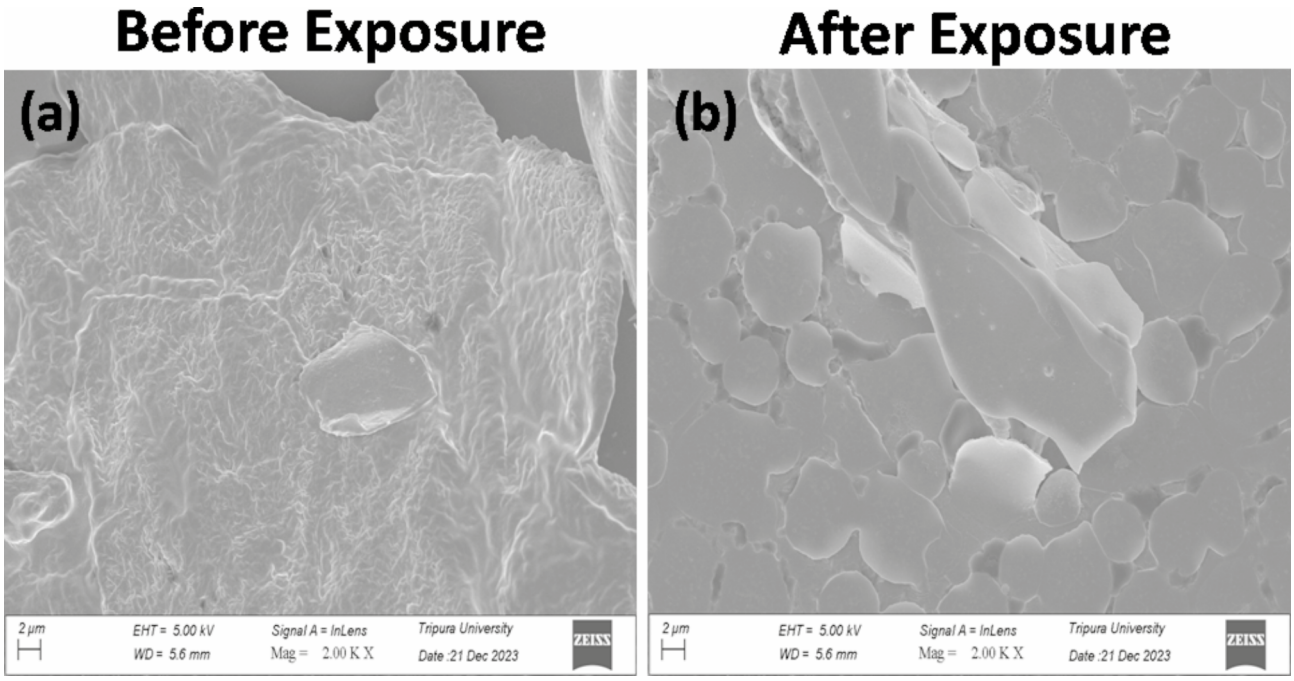

Fig. 11. FESEM images of (**a**) Acf + RhB (Concentrations are fixed at 10^{-4} M) and (**b**) Acf + RhB mixture after exposure to pretilachlor.

Conclusion

In summary, photophysical behavior of two dyes Acf and RhB assembled onto LbL films have been investigated under various conditions. It has been demonstrated that the material loss during LbL film formation can be minimized by incorporating clay mineral laponite. Similar approach can be used to minimize material loss in LbL films using other materials too. Temperature as well as pH dependant investigations indicate that Acf or RhB assembled onto the LbL films can be used to design either temperature sensor or pH sensor. FRET between Acf and RhB were also investigated successfully in presence and absence of different spacer molecules. Energy transfer occurred from Acf to RhB and the energy transfer efficiency increases in presence of clay laponite. On the other hand, the energy transfer efficiency decreases in presence of other spacers like SA, PAA etc. due to the increase in intermolecular separation between Acf and RhB. These results indicate that FRET between two molecules can be tuned incorporating spacer between them. It has also been observed that FRET between Acf

and RhB changes almost linearly with concentrations of a pesticide pretilachlor. This indicates that with proper calibration FRET between Acf and RhB can be used to design FRET based pretilachlor sensor with detection limit 0.22 ppm.

Data availability

Data is available upon request to the corresponding author (sahussain@tripurauniv.ac.in).

Received: 8 July 2024; Accepted: 27 December 2024
Published online: 22 January 2025

References

1. Nix, W. D. Mechanical properties of thin films. *Metall. Trans. A*. **20**, 2217–2245 (1989).
2. d'Auria, L., Huignard, J. P., Roy, A. M. & Spitz, E. Photolithographic fabrication of thin film lenses. *Opt. Commun.* **5**, 232–235 (1972).
3. *Handbook of Laser Technology and Applications*. (*Three- Volume Set)* 1675 (2003).
4. Hussain, S. et al. Tuning of polydiacetylene phase behavior mixed with cholesterol derivative and its application toward the detection of pathogenic bacteria. *J. Mater. Sci.* **58**, 15762–15779 (2023).
5. Rahman, F. Y. et al. Resistive switching behavior employing the Ipomoea carnea Plant for Biodegradable Rewritable read-only memory applications. *ACS Appl. Electron. Mater.* **5**, 3685–3697 (2023).
6. Yasmin Rahman, F. et al. Investigation of non volatile resistive switching behaviour using rose petal. *Materials Today: Proceedings* vol. 65 2693–2697 (2022).
7. Topasna, D. M. & Topasna, G. A. Numerical modeling of thin film optical filters. *Educ. Train. Opt. Photonics*. https://doi.org/10.1364/etop.2009.ep5 (2009).
8. Lee, C. C., Wan, D., Jaing, C. & Chu, C. Making aspherical mirrors by thin-film deposition. *Appl. Opt.* **32**, 5535 (1993).
9. Hassan-Aghaei, F. & Mohebi, M. M. Synthesis and characterization of novel multi-layer silica thin films with tailored mesostructure as anti-reflective coatings. *Opt. Mater.* **135**, 113246 (2023).
10. Tan, S. et al. Carbazole-based highly solid-state emissive fluorene derivatives with various mechanochromic fluorescence characteristics. *Dyes Pigm.* **177**, 108302 (2020).
11. Yin, Y. et al. Force-triggered hypso- and bathochromic bidirectional fluorescence switching beyond 120 nm and its anticounterfeiting applications. *Sci. Adv.* vol. 10 (2024).
12. Chen, Z. et al. Full-color Emissive D-D-A Carbazole luminophores: red-to-NIR Mechano-fluorochromism, aggregation-Induced Near-Infrared Emission, and application in photodynamic therapy. *Chem. – Eur. J.* **29** (2023).
13. Deb, R. et al. ZnO Nanoparticle-Induced performance enhancement of a coumarin-based nonvolatile memory device. *ACS Appl. Eng. Mater.* **2**, 1141–1152 (2024).
14. Dey, D. et al. Sensing of DNA conformation based on change in FRET efficiency between laser dyes. *Sens. Actuators B*. **204**, 746–753 (2014).
15. Lokhande, C. D. & Pawar, S. H. Electrodeposition of Thin Film Semiconductors. **16** January 17–40 (1989). https://doi.org/10.1515/9783112472866-004
16. Decher, G. Fuzzy nanoassemblies: toward layered polymeric multicomposites. *Science* **277**, 1232–1237 (1997).
17. Criado-Gonzalez, M., Mijangos, C. & Hernández, R. Polyelectrolyte Multilayer Films Based on Natural Polymers: From Fundamentals to Bio-Applications. *Polymers* vol. 13 2254 (2021).
18. Costa, Í. A., Maciel, A. P., Sales, M. J. A., Moreira, S. G. C. & Paterno, L. G. The Role played by Graphene Oxide in the Photodeposition and Surface-enhanced Raman scattering activity of Plasmonic Ag Nanoparticle substrates. *Phys. Status Solidi (a)* vol. 217 (2020).
19. Almeida, A. C., Vale, A. C., Pires, R. A., Reis, R. L. & Alves, N. M. Layer-by-layer films based on catechol-modified polysaccharides produced by dip- and spin-coating onto different substrates. *J. Biomedical Mater. Res. Part. B: Appl. Biomaterials*. **108**, 1412–1427 (2019).
20. Advincula, R., Aust, E., Meyer, W. & Knoll, W. In situ investigations of Polymer Self-Assembly Solution Adsorption by Surface Plasmon Spectroscopy. *Langmuir* **12**, 3536–3540 (1996).
21. Knoll, W. Self-assembled microstructures at interfaces. *Curr. Opin. Colloid Interface Sci.* **1**, 137–143 (1996).
22. Das, S. & Pal, A. J. Layer-by-Layer Self-Assembling of a Low Molecular Weight Organic Material by Different Electrostatic Adsorption Processes. *Langmuir* vol. 18 458–461 (2001).
23. Bhattacharjee, J., Banik, S., Hussain, S. A. & Bhattacharjee, D. A study on the interactions of cationic porphyrin with nano clay platelets in layer-by-layer (LbL) self assembled films. *Chem. Phys. Lett.* **633**, 82–88 (2015).
24. de Lima, L. F., Maciel, C. C., Ferreira, A. L., de Almeida, J. C. & Ferreira, M. Nickel (II) phthalocyanine-tetrasulfonic-Au nanoparticles nanocomposite film for tartrazine electrochemical sensing. *Mater. Lett.* **262**, 127186 (2020).
25. Rivero, P., Goicoechea, J. & Arregui, F. Layer-by-Layer Nano-assembly: A Powerful Tool for Optical Fiber Sensing Applications. *Sensors* vol. 19 683 (2019).
26. Kurapati, R., Groth, T. W. & Raichur, A. M. Recent developments in layer-by-layer technique for drug delivery applications. *ACS Appl. Bio Mater.* **2**, 5512–5527 (2019).
27. Caruso, F., Donath, E. & &Möhwald, H. Influence of Polyelectrolyte Multilayer Coatings on Förster Resonance Energy transfer between 6-Carboxyfluorescein and rhodamine B-Labeled particles in aqueous solution. *J. Phys. Chem. B*. **102**, 2011–2016 (1998).
28. Hu, Z., Huang, F. & Cao, Y. Layer-by-Layer Assembly of Multilayer Thin films for Organic Optoelectronic devices. *Small Methods* vol. 1 (2017).
29. Soh, S. et al. Layer-by-layer films for tunable and rewritable control of contact electrification. *Soft Matter*. **9**, 10233 (2013).
30. Costa, R. R. & Mano, J. F. Polyelectrolyte multilayered assemblies in biomedical technologies. *Chem. Soc. Rev.* **43**, 3453 (2014).
31. Dey, D., Bhattacharjee, D., Chakraborty, S. & Hussain, S. A. Effect of nanoclay laponite and pH on the energy transfer between fluorescent dyes. *J. Photochem. Photobiol., a.* **252**, 174–182 (2013).
32. Forster, T. Energiewanderung Und Fluoreszenz. *Die Naturwiss.* **33**, 166–175 (1946).
33. Főrster, T. 10th Spiers Memorial lecture. Transfer mechanisms of electronic excitation. Discuss. *Faraday Soc.* **27**, 7–17 (1959).
34. Hussain, S. A., Chakraborty, S., Bhattacharjee, D. & &Schoonheydt, R. A. Fluorescence Resonance Energy transfer between organic dyes adsorbed onto nano-clay and Langmuir–Blodgett (LB) films. *Spectrochim. Acta Part A Mol. Biomol. Spectrosc.* **75**, 664–670 (2010).
35. Hussain, S. A. et al. Fluorescence Resonance Energy Transfer (FRET) sensor. arXiv (2014). https://doi.org/10.48550/ARXIV.1408.6559
36. Verma, A. K., Noumani, A., Yadav, A. K. & Solanki, P. R. FRET Based Biosensor: Principle Applications Recent Advances and Challenges. *Diagnostics* vol. 13 1375 (2023).
37. Larkey, N. E. et al. Förster resonance energy transfer to impart signal-on and -off capabilities in a single microRNA biosensor. *Analyst* **141**, 6239–6250 (2016).

38. Prakash, S. & Verma, A. K. ANTHROPOGENIC ACTIVITIES AND BIODIVERSITY THREATS. *Int. J. Biol. Innovations*. **04**, 94–103 (2022).
39. Zhang, L. et al. A Sensitive and Specific Monoclonal Antibody Based Enzyme-Linked Immunosorbent Assay for the Rapid Detection of Pretilachlor in Grains and the Environment. *Foods* vol. 13 12 (2023).
40. Gao, L. et al. Selective magnetic solid-phase extraction of amide herbicides from fish samples coupled with ultra-high-performance liquid chromatography with tandem mass spectrometry. *J. Sep. Sci.* **45**, 896–907 (2021).
41. Deka, M. J. et al. Carbon dots derived from water hyacinth and their application as a sensor for pretilachlor. *Heliyon* **5**, e01985 (2019).
42. Liu, Z. J., Yu, P. M., Fang, S., Fan, J. & Wang, M. H. Development of an enzyme-linked immunosorbent assay for determination of pretilachlor in water and soil. *Ecotoxicol. Environ. Saf.* **74**, 1595–1599 (2011).
43. Takanishi, C. L., Bykova, E. A., Cheng, W. & Zheng J. GFP-based FRET analysis in live cells. *Brain Res.* **1091**, 132–139 (2006).
44. Szabó, T. et al. Adsorption of Protamine and Papain proteins on Saponite. *Clays Clay Miner.* **56**, 494–504 (2008).
45. Chen, Y., He, F., Ren, Y., Peng, H. & Huang, K. Fabrication of chitosan/PAA multilayer onto magnetic microspheres by LbL method for removal of dyes. *Chem. Eng. J.* **249**, 79–92 (2014).
46. Peruchon, L. et al. Characterization of self-cleaning glasses using Langmuir–Blodgett technique to control thickness of stearic acid multilayers. *J. Photochem. Photobiol., a*. **197**, 170–176 (2008).
47. Förster, T. ZwischenmolekulareEnergiewanderung Und Fluoreszenz. *Ann. Phys.* **437**, 55–75 (1948).
48. Berney, C. & Danuser, G. FRET or no FRET: a quantitative comparison. *Biophys. J.* **84**, 3992–4010 (2003).
49. de Villiers, M. M., Otto, D. P., Strydom, S. J. & Lvov, Y. M. Introduction to nanocoatings produced by layer-by-layer (LbL) self-assembly. *Adv. Drug Deliv. Rev.* **63**, 701–715 (2011).
50. Abdelaziz, B. B. et al. Spectral Behavior of a Conjugated Polymer MDMO-PPV Doped with ZnO Nanoparticles: Thin Films. *Nanomaterials* vol. 13 2405 (2023).
51. Borges, J. & Mano, J. F. Molecular interactions driving the layer-by-Layer Assembly of multilayers. *Chem. Rev.* **114**, 8883–8942 (2014).
52. Guzmán, E., Rubio, R. G. & Ortega, F. A closer physico-chemical look to the layer-by-layer electrostatic self-assembly of polyelectrolyte multilayers. *Adv. Colloid Interface Sci.* **282**, 102197 (2020).
53. Porcel, C. et al. From exponential to Linear Growth in Polyelectrolyte Multilayers. *Langmuir* **22**, 4376–4383 (2006).
54. Lavalle, P. et al. Comparison of the structure of Polyelectrolyte Multilayer films exhibiting a Linear and an Exponential Growth Regime: an in situ Atomic Force Microscopy Study. *Macromolecules* **35**, 4458–4465 (2002).
55. Elbert, D. L., Herbert, C. B. & Hubbell, J. A. Thin Polymer Layers Formed by Polyelectrolyte Multilayer Techniques on Biological Surfaces. *Langmuir* vol. 15 5355–5362 (1999).
56. Salomäki, M., Vinokurov, I. A. & Kankare, J. Effect of Temperature on the Buildup of Polyelectrolyte Multilayers. *Langmuir* vol. 21 11232–11240 (2005).
57. Sinek, A. et al. Temperature and pH-Dependent Response of Poly(Acrylic Acid) and Poly(Acrylic Acid-co-Methyl Acrylate) in Highly Concentrated Potassium Chloride Aqueous Solutions. *Polymers* vol. 12 486 (2020).
58. Shibanuma, T. et al. Thermosensitive phase-separation behavior of poly(acrylic acid)-graft-poly(N,N-dimethylacrylamide) aqueous solution. *Macromolecules* **33**, 444–450 (1999).
59. Banik, S. et al. Study of hysteresis during pH and temperature changes of Acriflavine: a gateway to Optrode. *Invertis J. Sci. Technol. vol.* **7.2**, 96–103 (2014).
60. Xu, K. et al. The polymeric conformational effect on capacitive deionization performance of graphene oxide/polypyrrole composite electrode. *Desalination* **486**, 114407 (2020).
61. Bignotti, F. Synthesis, characterisation and solution behaviour of thermo- and pH-responsive polymers bearing ?-leucine residues in the side chains. *Polymer* **41**, 8247–8256 (2000).
62. Dey, D., Islam, M. N., Hussain, S. A. & Bhattacharjee, D. Effect of temperature and ionic concentration on self-assembled films of Chicago Sky Blue. *Chin. Phys. Lett.* **25**, 3732–3734 (2008).
63. Sharma, V. K., Sahare, P. D., Rastogi, R. C., Ghoshal, S. K. & Mohan, D. Excited state characteristics of acridine dyes: acriflavine and acridine orange. *Spectrochim. Acta Part A Mol. Biomol. Spectrosc.* **59**, 1799–1804 (2003).
64. Muttaqien, S. E. et al. Photodynamic therapy using LCST polymers exerting pH-responsive isothermal phase transition. *J. Controlled Release*. **328**, 608–616 (2020).
65. Hussain, S. A., Roy, A. D., Saha, J., Dey, D. & Bhattacharjee, D. Effect of nano-clay platelet on fluorescence resonance energy transfer. *Invertis J. Renew. Energy*. **6**, 132 (2016).
66. Saha, J. et al. Development of arsenic(v) sensor based on fluorescence resonance energy transfer. *Sens. Actuators B*. **241**, 1014–1023 (2017).
67. Saha, J. et al. Investigation of fluorescence Resonance Energy transfer between Fluorescein and rhodamine 6G. *Spectrochim. Acta Part A Mol. Biomol. Spectrosc.* **149**, 143–149 (2015).
68. Schoonheydt, R. A. Smectite-Type Clay Minerals as nanomaterials. *Clays Clay Miner.* **50**, 411–420 (2002).
69. Saha, J., Dey, D., Roy, A. D., Bhattacharjee, D. & Hussain, S. A. Multi step FRET among three laser dyes Pyrene, Acriflavine and Rhodamine B. *J. Lumin.* **172**, 168–174 (2016).
70. Schoonheydt, R. A. Reflections on the material science of clay minerals. *Appl. Clay Sci.* **131**, 107–112 (2016).
71. Bunt, G. & Wouters, F. FRET from single to multiplexed signaling events. *Biophys. Rev.* **9**, 119–129 (2017).
72. Bene, L., Bagdány, M., Ungvári, T. & Damjanovich, L. Dual-laser tetra-polarization FRET (4polFRET) for site-selective control of Homo-FRET in Hetero-FRET systems on the cell surface: the Homo-FRET gate. *Anal. Chem.* **90**, 10159–10170 (2018).
73. Shrivastava, A. & Gupta, V. Methods for the determination of limit of detection and limit of quantitation of the analytical methods. *Chronicles Young Scientists*. **2**, 21 (2011).

Acknowledgements

S.A.H. acknowledges financial support from UGC-DAE-CSR (CRS/2022-23/04/912) and S.M acknowledges the scholarship under the UGC-DAE-CSR project (CRS/2022-23/04/912). The authors are also grateful to Central Instrumentation Centre, Tripura University for providing FESEM measurement facility. One of the authors, ANA acknowledges Research Institute Supporting Program (RICSP-24-1), King Saud University, Riyadh, Saudi Arabia.

Author contributions

Sangita Majumder: Conceptualization, Methodology, Data curation, Writing- Original draft. Subrata Deb: Conceptualization, Visualization, Investigation. Shazidul Hussain: Visualization, Data Curation. Dibyendu Dey: Data Curation, Visualization. Debajyoti. Bhattacharjee: Formal analysis, Validation. Abdullah N. Alodhayb: Investigation, Formal analysis. Shamima Hussain: Investigation, Formal analysis. Syed Arshad Hussain: Conceptualization, Supervision, Investigation, Writing- Original draft preparation.

Declarations

Competing interests
The authors declare no competing interests.

Additional information
Supplementary Information The online version contains supplementary material available at https://doi.org/10.1038/s41598-024-84846-7.

Correspondence and requests for materials should be addressed to S.A.H.

Reprints and permissions information is available at www.nature.com/reprints.

Publisher's note Springer Nature remains neutral with regard to jurisdictional claims in published maps and institutional affiliations.